Journal of Biomechanics 134 (2022) 111020

Contents lists available at ScienceDirect

Journal of Biomechanics

journal homepage: www.elsevier.com/locate/jbiomech

Predicting biological joint moment during multiple ambulation tasks

Jonathan Camargo *, Dean Molinaro, Aaron Young

Woodruff School of Mechanical Engineering, Georgia Institute of Technology, Atlanta, GA, USA
Institute for Robotics and Intelligent Machines (IRIM), Georgia Institute of Technology, Atlanta, GA, USA

ARTICLE INFO

Keywords:
Machine learning
Sensor-fusion
Biomechanics estimation
Joint moment prediction

ABSTRACT

Combining machine learning models with wearable sensing provides a key technique for understanding the biological effort, creating an alternative to inverse dynamics based on motion capture. In this study, we demonstrate a novel approach to not only estimate but predict the joint moment in advance for multiple ambulation modes. By combining electromyography (EMG), inertial measurement units (IMU), and electrogoniometers, we enable the prediction of the joint moment only from wearable sensors. We performed a forward feature selection to determine the best feature sets for different anticipation times of the intended moment generated at the hip, knee, and ankle, encompassing level walking on a treadmill and ascent/descent of stairs and ramps. We show that wearable sensors can predict the joint moment with an MAE of 0.06 ± 0.02 Nm/kg for direct estimation and an MAE of 0.10 ± 0.04 Nm/kg when predicting 150 ms in advance, corresponding to an MAE within 9.2% of the joint moment range. We found that the hip moment had a significantly lower error than the knee and ankle when anticipating the joint moment (Bonferroni test, $p < 0.05$). The accurate estimation of the joint moment could monitor user activity to reduce risk factors and inform the control of exoskeletons.

1. Introduction

Estimating the joint moments with wearable sensors allows the calculation of inverse dynamics on the fly, critical for outside of laboratory settings, where motion capture and force plates are not available. This information can be used in monitoring and reducing risk factors during locomotion, when lifting and handling materials, or during other physically demanding activities. Wearable robotics, such as exoskeleton technology, could use this information in real-time to improve controller decisions. The rationale is that devices operate at the joint level, and this output can inform the desired actuator torque. The instantaneous estimates of the user's intended joint moment could be used to directly shape the assistance control reference signal (Lenzi et al., 2013; Seo et al., 2016) or to map the assistance to a pre-optimized profile (Ding et al., 2018; Witte et al., 2020; Zhang et al., 2017). This method would require fewer tuning efforts, providing a more dynamic response(Gasparri et al., 2019).

Recent efforts have shown that it is possible to accurately estimate lower limb joint moments based on wearable sensors. Buchanan et al. used a forward dynamics model of the musculoskeletal system that uses the EMG signal to estimate joint moments (Buchanan et al., 2005). Similarly, other works have relied on system modeling (Jacobs and Ferris, 2015; Khurelbaatar et al., 2015; Sartori et al., 2012), requiring ground reaction forces to solve the inverse dynamics equations and a detailed description of the biomechanical system. Thus, other researchers have explored machine learning to eliminate the need to model inverse dynamics and, importantly, remove the need to measure external forces. Similar to the regression of any walking state parameter like speed (Zihajehzadeh and Park, 2016), altitude (Xia and Shi, 2020), or slope (Kang et al., 2019; Li et al., 2009), the process consists of setting the joint moment as a target for the inference in a supervised learning algorithm.

Wang et al. implemented a real-time estimation of the knee adduction moment using Neural Networks (NN) and XGBoost based on inertial measurement units (IMUs) (Wang et al., 2020). Xiong et al. showed that a NN could predict the joint moments during treadmill walking for the hip, knee, and ankle from electromyography (EMG) and goniometers (GON) (Xiong et al., 2019). However, the applications should extend beyond treadmill walking, given that community ambulation involves locomotion across different modes. In this study, we used machine learning to predict lower limb joint moments in three settings: level-ground treadmill, stair ascent/descent, and ramp ascent/descent. We used windowed feature extraction and machine learning for the regression of joint moment estimation from EMG, GON, and IMU

* Corresponding author.
E-mail address: jon-cama@gatech.edu (J. Camargo).

https://doi.org/10.1016/j.jbiomech.2022.111020
Accepted 21 February 2022
Available online 24 February 2022

spanning the entire lower limb.

In addition to joint moment estimation, we included a novel goal: predicting the intended joint moment. Using the information from the previous state of the sensors at a time t, we created models that predict the moment at a future time $t + \tau$, where the anticipation time τ represents how much forward in time the intended joint moment is predicted. The added benefit of predicting the joint moment forward in time is that potential controllers may include planning for the future torque requirements, rather than merely reacting, which allows for consideration of other factors, e.g., environmental and biological safety constraints (Zhang and Huang, 2019), or lag in the low-level controllers (He et al., 2019; Lund et al., 2019).

We studied how the anticipation time affects the error of the estimated joint moment and which sensors and features produce a lower prediction error. It can be expected that when the algorithms attempt to predict further ahead in time, the models' performance will decrease. However, we sought to determine what features would best mitigate this reduction in model performance. Given that some signals have a temporal correlation in terms of their causal interaction in the process of locomotion, we hypothesized that the anticipation of the joint moment would favor subsets of sensor signals. In particular, EMG data would be favored as it is a close measurement to the source of joint moment. Furthermore, as the EMG signal has a delay between muscle excitation and actual force production (Cavanagh and Komi, 1979) (i.e., electromechanical delay), we expect that anticipation time in the range of the electromechanical delay will increase the selection of EMG channels for predicting subject kinetics. Our work contributes to the field by: (1) showing that wearable sensors can predict the intended moment of multiple joints in different ambulation modes, (2) evaluating the influence of types of wearable sensing on the prediction through a forward channel selection.

2. Methods

2.1. Data collection

Data for biomechanics and wearable sensors from N = 12 subjects (8 males, 4 females, age 20.6 ± 1.5 yr., mass 68.9 ± 13.6 kg, height 1.71 ± 0.08 m) were collected in a study approved by the Institutional Review Board at the Georgia Institute of Technology Protocol No.H17240. Inclusion criteria corresponded to able-bodied adults without conditions that affected mobility. The subjects were instrumented with wearable sensors measuring accelerometer and gyroscopic data from inertial measurement units (IMUs) sampled at 100 Hz (Yost LX embedded, Yost, Ohio, US), surface electromyography sampled at 1000 Hz (EMG) (Biometrics datalink DLK900, Biometrics Ltd, UK), joint angles and their change rate were measured with electrogoniometers sampled at 1000 Hz (GON) (Biometrics datalink DLK900, Biometrics Ltd, UK). IMUs were placed on each segment of the lower limb and on the trunk. EMG sensors were attached to major muscle groups (Gluteus Medius, Vastus Lateralis and Medialis, Rectus Femoris, Biceps Femoris, Semitendinosus, Gracilis, Soleus, Tibialis Anterior, Gastrocnemius Medialis, and Right External Oblique) and electrogoniometers were attached to the hip, knee, and ankle, capturing sagittal plane angles as well as the frontal plane angle of the ankle (Fig. 1). Subjects performed 5 trials of ascent and descent on stairs with 4 different step heights of 10.16 cm (4in), 12.70 cm (5in), 15.24 cm (6in), and 17.78 cm (7in) for a total of 20 stair trials. Subjects performed 5 trials of ramp ascent and descent on 6 different slopes of 5.2°, 7.8°, 9.2°, 11°, 12.4°, and 18° for a total of 30 ramp trials.

Finally, subjects performed 15 min of walking on a treadmill at 28 different speeds, from 0.5 to 1.85 m/s. Biomechanics data were computed from motion capture following the Helen Hayes Hospital using OpenSim (Delp et al., 2007). Forceplate data, including GRF and CoP, were recorded at 1000 Hz on the instrumented split treadmill (Bertec, Columbus, US) and forceplates inserts (4060-05, Bertec, Columbus, US) placed in-ground at the mid-section of the ramp and each step of the staircase. Sensor data were synchronized with motion capture marker data using a Vicon Lock synchronization box (Vicon Motion Systems, UK).

We used the Gait2354_Simbody model, scaled to the segment dimensions of each subject. Then, we used subject models with the inverse kinematics and inverse dynamics tools to generate the joint angles and compute the joint moments from motion capture and force plate data filtered with a 6 Hz Butterworth lowpass filter. Although the 3D kinetic

Sensor type	Measured channels	Sensor location
Goniometers (GON)	Joint angle Rate of change ('d_')	Hip
		Knee
		Ankle
Inertial Measurement Units (IMU)	Accelerometer XYZ Gyroscope XYZ	Trunk
		Thigh
		Shank
		Foot
Electromyography (EMG)	Surface EMG at targeted muscle	Gastrocnemius medialis
		Tibialis anterior
		Soleus
		Vastus medialis
		Vastus lateralis
		Rectus femoris
		Biceps femoris
		Semitendinosus
		Gracilis
		Gluteus medius
		Right external oblique

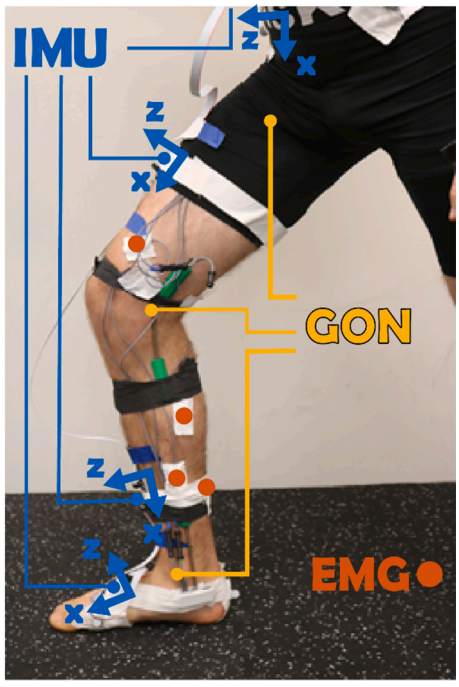

Fig. 1. Sensor placement. EMG electrodes were placed on the lower limb, targeting the major muscle groups. Goniometers were placed at the hip, knee, ankle joint. IMUs were placed on each segment of the lower limb and the torso.

analysis generates abduction/adduction hip moment, our focus was the prediction of the flexion/extension moments at the hip, knee, and ankle. These joint moments were normalized by subject mass (Nm/kg) and considered as the ground truth for the supervised training of the models.

2.2. Model selection

We limited the scope of the analysis to two types of models: feed-forward NN and XGBoost. NNs are extensively used in locomotion recognition and parameter estimation (Aminian et al., 1994; Mannini and Sabatini, 2014). XGBoost is an algorithm based on gradient boosting and ensemble learning (Chen and Guestrin, 2016). It has shown excellent performance with low model complexity and training times (Bhakta et al., 2020; Lu et al., 2019). The hyperparameters of XGBoost and the NN architecture were selected based on previous work in which we achieved biological hip moment estimation (Molinaro et al., 2020). We used a maximum depth of 6 for the XGBoost, while we used a fully connected network with 2 hidden layers (size 10) and *tanh* activation for the NN models.

2.3. Feature engineering and selection

We processed the raw time-series data using a sliding window scheme for feature extraction (Hudgins et al., 1993; Lotte, 2012). The process consists of using a fixed-size window to compute signal characteristics in an interval before the event to be predicted. For every window of data, we computed a total of 675 features, as described in Table 1. Data windows were updated with a sliding step of 10 ms for a targeted refresh rate of 100 Hz. We selected 250 ms as the window size based on a preliminary evaluation of the effect of window size on the moment error. We determined that window sizes between 100 ms and 400 ms had no significant effect on the error.

We defined the anticipation time as the difference between the time of the last sample in the window and the time when the joint moment is predicted (Fig. 2). For anticipation times between 0 ms and 250 ms with increments of 10 ms, we determined the error of the predicted moment for each of the three joints in the lower limb: hip, knee, and ankle. Our approach was to run a sequential forward feature selection to establish the features that optimally reduce the error using a greedy search. We independently ran the feature selection for each anticipation time to determine the best features and their corresponding performance, defined by the mean absolute error of the joint moment. Thus, our analysis encompassed the evaluation of the best features to predict the joint moment at each case of the independent variables: joints (hip, knee, ankle), ambulation modes (treadmill, stair, ramp), and anticipation times (0 to 250 ms).

To guarantee that testing data never included training data, cross-validation based on trial index was performed as follows. The 5 trials performed per condition in stairs and ramps were enumerated from 1 to 5. The 15-minutes trial for treadmill walking was split into 5 sections of 3 min and enumerated from 1 to 5. Then, we used each trial index from 1 to 5 to create k = 5 folds for cross-validation. Within each fold *i*, feature tables from the trial of index *i*, were preserved as testing data and the remaining trials as training data. Models were trained per subject using the training data of each fold and evaluated with the corresponding testing data. On each inclusion step of the forward feature selection, we determine the next best feature to include, defined as the one that provided the least average error across subjects.

Due to the significant computational demands of a forward feature selection process, we limited the maximum number of features to be included in the selection to 32. This number was established by evaluating 18 boundary cases of the independent variables (i.e., minimum and maximum anticipation time for each combination of joint and ambulation mode). No considerable reduction of the model error occurred when adding more than 32 features.

Table 1
Features computed per channel for each window of data.

Feature	Description
Autoregression Coefficients (Order 6)	Coefficients of the Levinson-Durbin recursion. (*levinson*)
Slope Sign Changes	*sum(abs(diff(diff(data_window) > 0)))*
Zero Crossings	*sum(abs(diff(data_window > 0)))*
Mean	*sum(data_window)/numel(data_window)*
Root Mean Square (RMS)	*rms(data_window)*
Minimum	min*(data_window)*
Maximum	max*(data_window)*
Waveform Length	*sum(abs(diff(data_window)))*
Mean Absolute Value	*sum(abs(data_window))/numel(data_window)*
Standard Deviation	*std(data_window)*

2.4. Statistical analysis

We used a *t*-test to evaluate the difference between XBGoost and NN regarding the number of features needed. We used quadratic regression to study the effects of the anticipation time on the error of moment prediction per joint. We used repeated-measures ANOVA (RM-ANOVA) to evaluate the effect of model types, joints and ambulation modes on the prediction error. Main effect comparisons were performed with post-hoc t-tests using the family-wise Bonferroni method to correct for multiple comparisons, reporting the p-value after correction. Finally, we determined the sensors' role by observing the number of different signal types selected at each anticipation time and the contribution to error. The statistical analyses were evaluated with a 95% confidence interval and a significance level $\alpha = 0.05$ using the software Minitab 19.

3. Results

3.1. Convergence of the feature selection process

For both model types, the feature selection showed convergence to a minimum error when increasing the features (Fig. 3). No significant difference was found for the number of features required between the XGBoost model (10.3 ± 1.2 features) and the NN (10.1 ± 1.8 features) for convergence of MAE within 5% error (*t*-test, $p = 0.12$). With this result, an input vector size of 11 features was used for the subsequent analyses. The XGBoost algorithm did not suffer from a loss in accuracy compared to the NN with a large number of features in the model.

3.2. Prediction of joint moment

For all the joints and modes, the trained models could predict the joint moment using only 11 inputs, with an average MAE of 0.06 ± 0.02 Nm/kg for XGBoost, and an average MAE of 0.07 ± 0.01 Nm/kg for NN in the 0 ms case. The prediction forward in time of the moment introduces an increase in error proportional to the anticipation time. As an example, Fig. 4 illustrates the tracking of the moment produced, observing increased deviations from the ground truth as the prediction increases. The highest error was found for the highest anticipation time (250 ms) with an average MAE of 0.11 ± 0.04 Nm/kg for XGBoost, and an average MAE of 0.12 ± 0.05 Nm/kg for NN. However, as observed in Fig. 5, even though the error increased with the anticipation time, the rate of increase in error with respect to the prediction for the hip ($\beta_1 = 0.14 \pm 0.07$ Nm/kg s) was consistently less than that of the knee ($\beta_1 = 0.44 \pm 0.17$ Nm/kg s) and ankle joint moment ($\beta_1 = 0.38 \pm 0.18$ Nm/kg s).

In general, the error of the predicted moment in the same order of magnitude for all the joints and ambulation modes. Yet, the prediction of the joint moment for treadmill walking was consistently more accurate than ramp and stair ambulation (Bonferroni test, $p < 0.05$). No significant difference was found between the NN and XGBoost models (RM-ANOVA, $p = 0.10$).

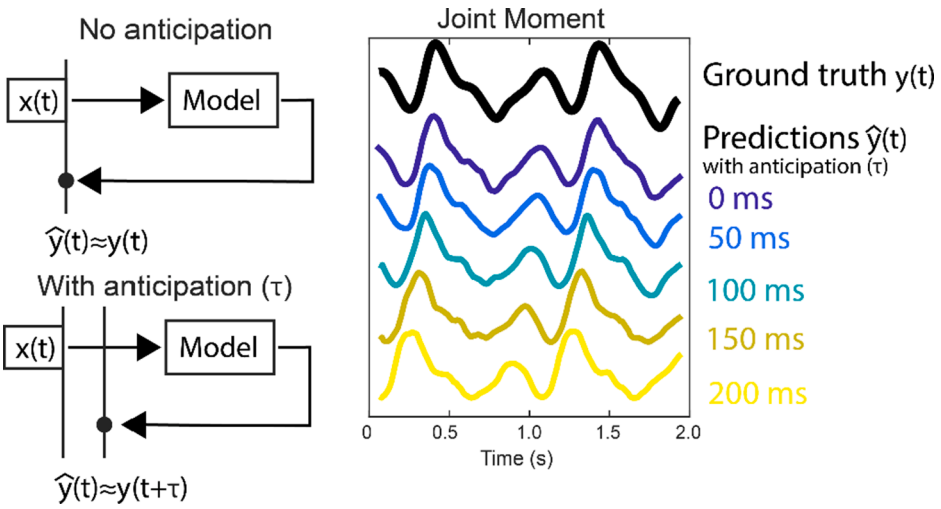

Fig. 2. Prediction of the joint moment. At the instant t, the feature vector x(t) is computed using the last window of samples. Models are trained to produce $\hat{y}$ as predictions of the ground truth joint moment. The models can be trained to anticipate the joint moment signal at a future time $t + \tau$, where τ **is** defined as the anticipation time.

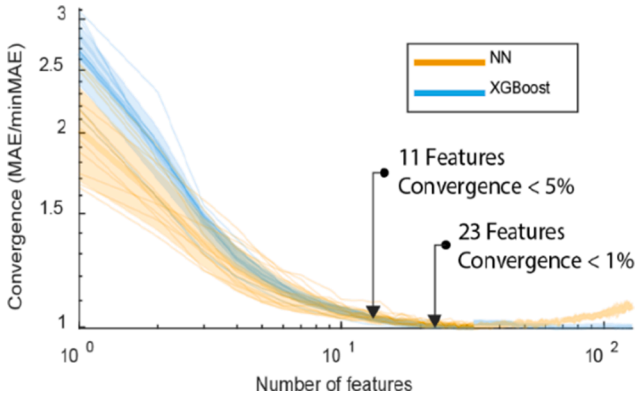

Fig. 3. Convergence of the error in the feature selection process. The bold line shows the normalized error, defined as the error of each iteration divided by the minimum error obtained in the feature selection process. The shaded area represents the standard deviation. Including more features in the model reduces the error with an improvement of less than 5% after 11 features and an improvement of 1% after 23 features.

3.3. Channels selected

Since we found a slightly lower error for XGBoost models, we focused on this model to observe the most important trends in the feature selection as a function of the anticipation time. Fig. 6. presents the percentage of types of sensors (IMU, EMG, and GON) included by the feature selection for each joint and ambulation mode, grouped by 50 ms intervals of anticipation time. On average across all joints, ambulation modes and anticipations, IMU and GON sensors encompassed 38.9% and 38.4% of the selected features, respectively. On the other hand, EMG corresponded, on average, to 22.6% of the selected features. For greater anticipation times (>150 ms), EMG was not selected to predict the hip moment on treadmill and showed reduced influence in all ambulation modes for the knee joint. On average, EMG comprised 26.3% of the selected features for anticipation times up to 150 ms and only 16.8% of the selected features for greater anticipation times.

The type of channels selected present variations depending on the anticipation time (Fig. 6). The hip moment prediction was realized mainly from the hip GON, knee GON, and thigh IMU gyroscopic signals across all the anticipation times. The EMG of the soleus was included throughout all anticipation times, and the EMG of the vastii muscles was included only for the range of 0–150 ms. The prediction of the knee moment had a spread distribution, including knee GON, hip GON, ankle GON, and soleus EMG for all the anticipation times. The Vastii muscles

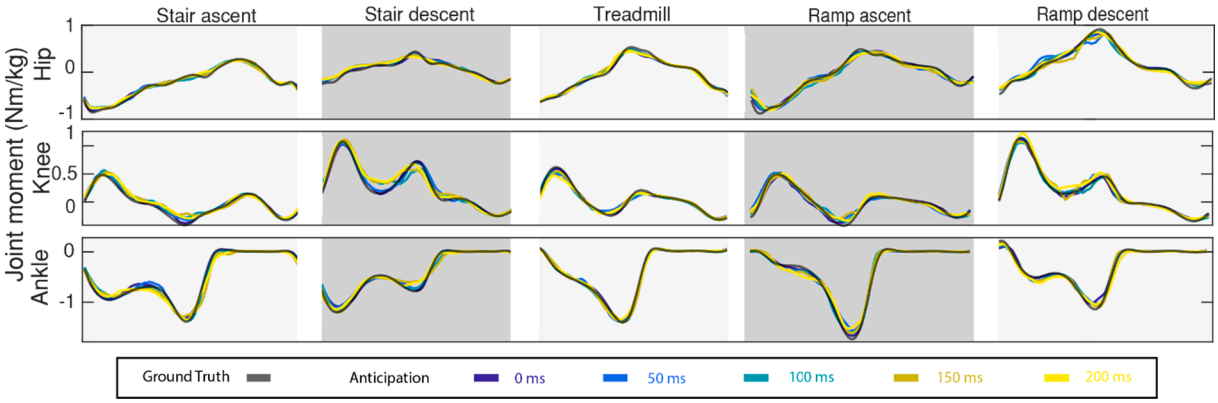

Fig. 4. Single stride examples of the prediction of joint moments during locomotion in multiple ambulation modes and different anticipation times using XGBoost. Note that the predicted moments were aligned to the corresponding future time of the ground truth signal. The error of the prediction increases as the model attempts to predict the torque further in time.

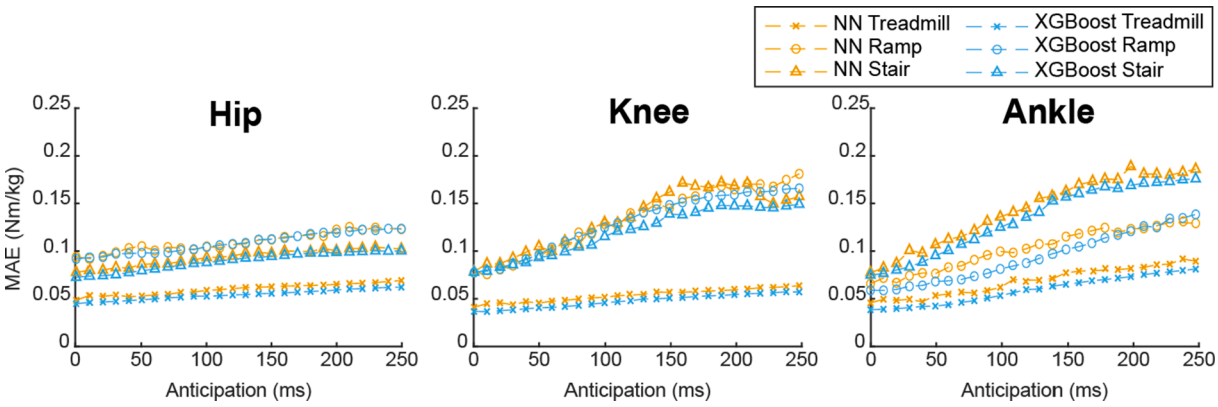

Fig. 5. Mean absolute error (MAE) for estimating the joint moment at different levels of prediction and three different ambulation modes (stair, ramp, treadmill). The best accuracy is produced when no prediction is attempted (average MAE 0.06Nm/kg for XGBoost, 0.07Nm/kg for NN). The prediction of the hip moment is less sensitive to the anticipation time compared to the prediction of the knee and ankle moments, The moment prediction is significantly more accurate for walking on treadmill than on ramps or stairs (Bonferroni test, $p < 0.05$).

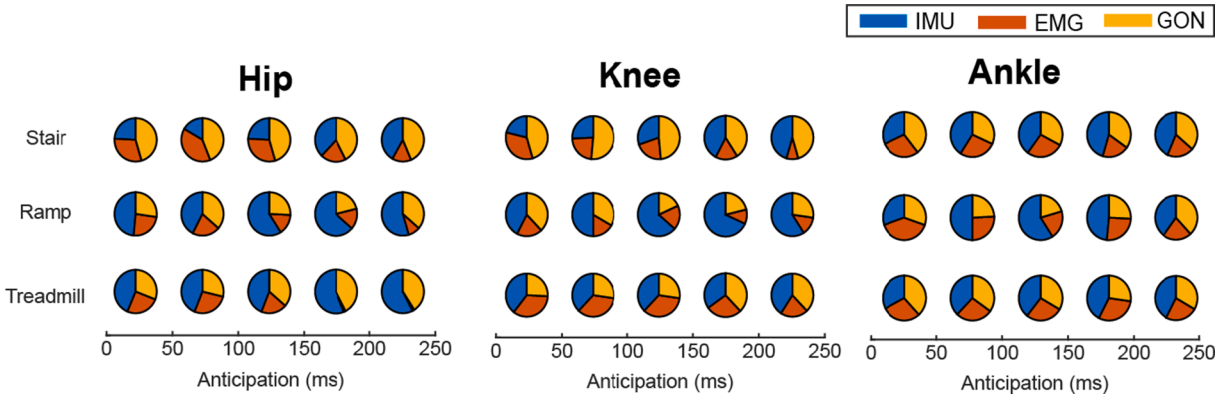

Fig. 6. Distribution of the 11 selected inputs for XGBoost among the categories: IMU, EMG, GON. The results are aggregated in intervals of 50 ms in the anticipation time. Features related to EMG were consistently influential in the ankle moment's prediction, comprising 27.2% of the selected features on average. Fewer EMG features were selected as the anticipation time increased for the knee and hip, observing 24.6% of EMG features for anticipation time under 150 ms and 13.3% EMG features for anticipation time over 150 ms.

were also selected in the range of 0–150 ms for this joint. The ankle moment presents more influence from the EMG, including gastrocnemius medialis for the full range of the anticipation times. For this joint, the foot IMU gyroscope was the channel predominantly selected. The detailed distribution of channels selected is presented in Supplemental Figs. S.1.1-S1.3.

4. Discussion

Online joint kinetics estimation has been achieved using different methods, including inverse dynamics modeling and ground reaction force measurements. This study used conventional sensors that are common to wearable robotics without requiring the addition of instrumented insoles as a means to capture ground reaction forces (Jacobs and Ferris, 2015; Khurelbaatar et al., 2015). Our work expands the ambulation modes from previous literature to include predicting joint moments in ramps and stairs, demonstrating that this technique can work in different settings. Furthermore, we proposed predicting the joint moment forward in time so that potential wearable robotic controllers benefit from planning instead of reacting to the user's torque.

As expected, increasing the anticipation time came with the expense of a rise in the error. However, the worst MAE up to 150 ms remained below 0.10 Nm/kg, corresponding to the ankle in stairs locomotion and representing 9.2% of the ankle moment range. This error level is comparable to modeling-based methods that do not anticipate the joint moment. For reference, Forner-Cordero et al. used inverse dynamics modeling from insole contact force, finding 0.15 Nm/kg RMSE (Forner-Cordero et al., 2006); other methods included modeling the muscle state and dynamics based on EMG (Sartori et al.: 0.20 Nm/kg MAE (Sartori et al., 2012), Buchanan, et al.: 0.10 Nm/kg RMSE (Buchanan et al., 2005)). Additionally, none of these methods attempted to predict future joint moments as done in this study. Thus, the results suggest that the machine learning-based approach offers lower error. For reference, our 0 ms prediction XGBoost MAE of 0.06 Nm/kg nearly halves the error level of the reported methods based on dynamics modeling with wearables.

In comparison to the knee and ankle joints, the predictions of the hip moment have less increase in error when anticipating further in time. This finding is potentially explained by the reduced variability in the kinematics and kinetics of the hip joint during locomotion as opposed to the other joints (Smith, 1993). The same effect occurs when comparing the moment prediction on the treadmill with respect to stairs and ramps. We found that the treadmill error was 40% less than the error in the other ambulation modes. This can be explained since the consistent speed reduces the variability across steps, as reported in previous studies that evaluate spatiotemporal and kinematic parameters (Dingwell et al., 2001; Terrier, 2012; Wiens et al., 2019). For example, Dingwell et al. reported a significant reduction of the standard deviation of lower extremity kinematics on the treadmill versus walking overground (Dingwell et al., 2001).

We did not find any significant difference in model error between XGBoost and NN. Observing that these general-purpose algorithms can predict joint moments with as little as 11 inputs is promising, as it reduces the size of the required training datasets and eliminates the need for synthetic data, as opposed to more complex techniques such as Convolutional Neural Networks (Dorschky et al., 2020). The algorithms did not show any significant improvement when increasing the number of inputs, showing a feature selection convergence within 1% for 23 features. In fact, for the NN models, exceeding the number of features caused increased model error due to overfitting.

We evaluated the most influential channels of sensor data that are required to predict joint moments, finding a substantial effect from the anticipation time, the target joint, and ambulation mode. Primarily, the prediction of ankle moment favored EMG data, with the soleus and gastrocnemius used across all anticipation times. On the other hand, the hip and knee joint moment predictions were influenced less by the EMG for the greater anticipation times (over 150 ms).

As it creates a lag between the muscle activation and the actual force production, the electromechanical delay affects the channel selection and may explain the lack of model preference for EMG channels for greater anticipation times. For example, the vastus lateralis, with in vivo electromechanical delay of around 90 ms (Vos et al., 1990), would provide more direct information for the estimation of the hip and knee moment around 90 ms in advance. This was observed in the consistent inclusion of the vastus lateralis for knee moment estimation within 50 to 150 ms in all the ambulation modes (Supplemental Figs. S1.1-S1.3). Another aspect of interest is that the channels that carry information from other segments and joints get selected more as the anticipation time was increased, whereas 0 ms prediction tended to favor more local sensing at the joint. For example, predicting future moment at the knee involved signals such as forward foot acceleration and ankle sagittal angle. This is a potential effect of the model effort to exploit the system dynamics' coupling.

This study provides an overview of the influence of various sensors to predict the joint moment, finding trends that are shared across subjects. While this analysis allows the reduction of the features and sensor sets for a particular joint or ambulation mode, the results showed that combining multiple sensor types is still required to achieve lower error. This could hinder the deployment in applications outside of research laboratories. We consider that developments in smart textiles and low-profile wearable sensing could mitigate this limitation (Wicaksono et al., 2020).

Another limitation of this study is that the models were trained on a subject-by-subject basis per ambulation mode. Thus, the error metrics obtained may not be representative of testing pre-trained models on novel users or dynamic mode changes. Furthermore, the moment estimation could be beneficial in clinical settings to inform assistive devices in populations with balance impairments. However, these populations may exhibit ambulation patterns that differ from the healthy subject population evaluated in this work and require further study, nevertheless applying similar analysis to the reported here. Additionally, including robotic assistance from a wearable device can alter biomechanical patterns and signal levels, influencing the model's performance. Future work will focus on evaluating the moment prediction response in applications of robotic assistance and exploring the implementation of subject-independent models.

CRediT authorship contribution statement

Jonathan Camargo: Conceptualization, Data curation, Formal analysis, Investigation, Methodology, Visualization, Writing – original draft, Writing – review & editing. **Dean Molinaro:** Conceptualization, Data curation, Formal analysis, Writing – original draft, Writing – review & editing. **Aaron Young:** Writing – review & editing, Supervision, Resources, Project administration, Methodology, Funding acquisition, Conceptualization.

Declaration of Competing Interest

The authors declare that they have no known competing financial interests or personal relationships that could have appeared to influence the work reported in this paper.

Acknowledgments

This work was supported by a Fulbright fellowship awarded to Jonathan Camargo-Leyva. The NSF NRI Award also funded this research under No. 1830215, the National Science Foundation Graduate Research Fellowship under Grant No. DGE-1650044, and the NRT: Accessibility, Rehabilitation, and Movement Science (ARMS) Award No. 1545287.

Appendix A. Supplementary material

Supplementary data to this article can be found online at https://doi.org/10.1016/j.jbiomech.2022.111020.

References

Aminian, K., Robert, P., Jéquier, E., Schutz, Y., 1994. Estimation of speed and incline of walking using neural network. *Conference Proceedings - 10th Anniv., IMTC 1994: Advanced Technologies in I and M. 1994 IEEE Instrumentation and Measurement Technology Conference*, *44*(3), 160–162. https://doi.org/10.1109/IMTC.1994.352073.

Bhakta, K., Camargo, J., Donovan, L., Herrin, K., Young, A., 2020. Machine Learning Model Comparisons of User Independent & Dependent Intent Recognition Systems for Powered Prostheses. IEEE Rob. Autom. Lett. 5 (4), 5393–5400. https://doi.org/10.1109/LRA.2020.3007480.

Buchanan, T.S., Lloyd, D.G., Manal, K., Besier, T.F., 2005. Estimation of muscle forces and joint moments using a forward-inverse dynamics model. Med. Sci. Sports Exerc. 37 (11), 1911–1916. https://doi.org/10.1249/01.mss.0000176684.24008.6f.

Cavanagh, P.R., Komi, P.V., 1979. Electromechanical delay in human skeletal muscle under concentric and eccentric contractions. Eur. J. Appl. Physiol. 42 (3), 159–163. https://doi.org/10.1007/BF00431022.

Chen, T., Guestrin, C., 2016. XGBoost: A Scalable Tree Boosting System. *Proceedings of the 22nd ACM SIGKDD International Conference on Knowledge Discovery and Data Mining*, *1*(1), 785–794.

Delp, S.L., Anderson, F.C., Arnold, A.S., Loan, P., Habib, A., John, C.T., Guendelman, E., Thelen, D.G., 2007. OpenSim: Open-Source Software to Create andAnalyze Dynamic Simulations of Movement. IEEE Trans. Bio-Med. Eng. 54 (11), 1940–1950. https://doi.org/10.1109/TBME.2007.901024.

Ding, Y., Kim, M., Kuindersma, S., Walsh, C.J., 2018. Human-in-the-loop optimization of hip assistance with a soft exosuit during walking. Sci. Rob. 3 (15), 1–9. https://doi.org/10.1126/scirobotics.aar5438.

Dingwell, J.B., Cusumano, J.P., Cavanagh, P.R., Sternad, D., 2001. Local dynamic stability versus kinematic variability of continuous overground and treadmill walking. J. Biomech. Eng. 123 (1), 27–32. https://doi.org/10.1115/1.1336798.

Dorschky, E., Nitschke, M., Martindale, C.F., van den Bogert, A.J., Koelewijn, A.D., Eskofier, B.M., 2020. CNN-Based Estimation of Sagittal Plane Walking and Running Biomechanics From Measured and Simulated Inertial Sensor Data. Front. Bioeng. Biotechnol. 8 (June), 1–14. https://doi.org/10.3389/fbioe.2020.00604.

Forner-Cordero, A., Koopman, H.J.F.M., Van Der Helm, F.C.T., 2006. Inverse dynamics calculations during gait with restricted ground reaction force information from pressure insoles. Gait Posture 23 (2), 189–199. https://doi.org/10.1016/j.gaitpost.2005.02.002.

Gasparri, G.M., Luque, J., Lerner, Z.F., 2019. Proportional Joint-Moment Control for Instantaneously Adaptive Ankle Exoskeleton Assistance. IEEE Trans. Neural Syst. Rehabil. Eng. 27 (4), 751–759. https://doi.org/10.1109/TNSRE.2019.2905979.

He, B., Thomas, G.C., Paine, N., Sentis, L., 2019. Modeling and loop shaping of single-joint amplification exoskeleton with contact sensing and series elastic actuation. *Proceedings of the American Control Conference*, *2019-July*, 4580–4587. https://doi.org/10.23919/acc.2019.8814421.

Hudgins, B., Parker, P., Scott, R.N., 1993. A New Strategy for Multifunction Myoelectric Control. IEEE Trans. Biomed. Eng. 40 (1), 82–94. https://doi.org/10.1109/10.204774.

Jacobs, D.A., Ferris, D.P., 2015. Estimation of ground reaction forces and ankle moment with multiple, low-cost sensors. J. NeuroEng. Rehabil. 12 (1), 1–12. https://doi.org/10.1186/s12984-015-0081-x.

Kang, I., Kunapuli, P., Hsu, H., Young, A.J., 2019. Electromyography (EMG) signal contributions in speed and slope estimation using robotic exoskeletons. *IEEE International Conference on Rehabilitation Robotics*, *2019-June*, 548–553. https://doi.org/10.1109/ICORR.2019.8779433.

Khurelbaatar, T., Kim, K., Lee, S.K., Kim, Y.H., 2015. Consistent accuracy in whole-body joint kinetics during gait using wearable inertial motion sensors and in-shoe pressure sensors. Gait Posture 42 (1), 65–69. https://doi.org/10.1016/j.gaitpost.2015.04.007.

Lenzi, T., Carrozza, M.C., Agrawal, S.K., 2013. Powered hip exoskeletons can reduce the user's hip and ankle muscle activations during walking. IEEE Trans. Neural Syst. Rehabil. Eng. 21 (6), 938–948. https://doi.org/10.1109/TNSRE.2013.2248749.

Li, Q., Young, M., Naing, V., Donelan, J.M., 2009. Walking speed and slope estimation using shank-mounted inertial measurement units. *2009 IEEE International Conference on Rehabilitation Robotics, ICORR 2009*, 839–844. https://doi.org/10.1109/ICORR.2009.5209598.

Lotte, F., 2012. A new feature and associated optimal spatial filter for EEG signal classification: Waveform Length. *Pattern Recognition (ICPR), 2012 21st International …*, *Icpr*, 2–5. https://doi.org/10.0/Linux-x86_64.

Lu, H., Pinaroc, M., Lv, M., Sun, S., Han, H., Shah, R.C., 2019. Locomotion recognition using XGboost and neural network ensemble. *UbiComp/ISWC 2019- - Adjunct Proceedings of the 2019 ACM International Joint Conference on Pervasive and Ubiquitous Computing and Proceedings of the 2019 ACM International Symposium on Wearable Computers*, 757–760. https://doi.org/10.1145/3341162.3344870.

Lund, S.H.J., Billeschou, P., Larsen, L.B., 2019. High-bandwidth active impedance control of the proprioceptive actuator design in dynamic compliant robotics. Actuators 8 (4), 1–33. https://doi.org/10.3390/ACT8040071.

Mannini, A., Sabatini, A.M., 2014. Walking speed estimation using foot-mounted inertial sensors: Comparing machine learning and strap-down integration methods. Med. Eng. Phys. 36 (10), 1312–1321. https://doi.org/10.1016/j.medengphy.2014.07.022.

Molinaro, D.D., Kang, I., Camargo, J., Young, A.J., 2020. *Biological Hip Torque Estimation using a Robotic Hip Exoskeleton*. 791–796. https://doi.org/10.1109/biorob49111.2020.9224334.

Sartori, M., Reggiani, M., Farina, D., Lloyd, D.G., Gribble, P.L., 2012. EMG-Driven Forward-Dynamic Estimation of Muscle Force and Joint Moment about Multiple Degrees of Freedom in the Human Lower Extremity. PLoS ONE 7 (12), e52618. https://doi.org/10.1371/journal.pone.0052618.

Seo, K., Lee, J., Lee, Y., Ha, T., Shim, Y., 2016. Fully autonomous hip exoskeleton saves metabolic cost of walking. *Proceedings - IEEE International Conference on Robotics and Automation*, *2016-June*, 4628–4635. https://doi.org/10.1109/ICRA.2016.7487663.

Smith, A., 1993. Variability in human locomotion: are repeat trials necessary? Australian J. Physiotherapy 39 (2), 115–123. https://doi.org/10.1016/S0004-9514(14)60476-1.

Terrier, P., Thomas, A.LR., 2012. Step-to-Step Variability in Treadmill Walking: Influence of Rhythmic Auditory Cueing. PLoS ONE 7 (10), e47171. https://doi.org/10.1371/journal.pone.0047171.

Vos, E.J., Mullender, M.G., van Ingen Schenau, G.J., 1990. Electromechanical delay in the vastus lateralis muscle during dynamic isometric contractions. Eur. J. Appl. Physiol. 60 (6), 467–471. https://doi.org/10.1007/BF00705038.

Wang, C., Chan, P.P.K., Lam, B.M.F., Wang, S., Zhang, J.H., Chan, Z.Y.S., Chan, R.H.M., Ho, K.K.W., Cheung, R.T.H., 2020. Real-Time Estimation of Knee Adduction Moment for Gait Retraining in Patients with Knee Osteoarthritis. IEEE Trans. Neural Syst. Rehabil. Eng. 28 (4), 888–894. https://doi.org/10.1109/TNSRE.2020.2978537.

Wicaksono, I., Tucker, C.I., Sun, T., Guerrero, C.A., Liu, C., Woo, W.M., Pence, E.J., Dagdeviren, C., 2020. A tailored, electronic textile conformable suit for large-scale spatiotemporal physiological sensing in vivo. NPJ Flexible Electron. 4 (1) https://doi.org/10.1038/s41528-020-0068-y.

Wiens, C., Denton, W., Schieber, M.N., Hartley, R., Marmelat, V., Myers, S.A., Yentes, J. M., 2019. Walking speed and spatiotemporal step mean measures are reliable during feedback-controlled treadmill walking; however, spatiotemporal step variability is not reliable. J. Biomech. 83, 221–226. https://doi.org/10.1016/j.jbiomech.2018.11.051.

Witte, K.A., Fiers, P., Sheets-Singer, A.L., Collins, S.H., 2020. Improving the energy economy of human running with powered and unpowered ankle exoskeleton assistance. Sci. Rob. 5 (40) https://doi.org/10.1126/scirobotics.aay9108.

Xia, M., Shi, C., 2020. Autonomous Pedestrian Altitude Estimation Inside a Multi-Story Building Assisted by Motion Recognition. IEEE Access 8, 104718–104727. https://doi.org/10.1109/ACCESS.2020.3000313.

Xiong, B., Zeng, N., Li, H., Yang, Y., Li, Y., Huang, M., Shi, W., Du, M., Zhang, Y., 2019. Intelligent Prediction of Human Lower Extremity Joint Moment: An Artificial Neural Network Approach. IEEE Access 7, 29973–29980. https://doi.org/10.1109/ACCESS.2019.2900591.

Zhang, J., Fiers, P., Witte, K.A., Jackson, R.W., Poggensee, K.L., Atkeson, C.G., Collins, S. H., 2017. Human-in-the-loop optimization of exoskeleton assistance during. Sci. Rob. 1284 (June), 1280–1284.

Zhang, T., Huang, H.e., 2019. Design and Control of a Series Elastic Actuator with Clutch for Hip Exoskeleton for Precise Assistive Magnitude and Timing Control and Improved Mechanical Safety. IEEE/ASME Trans. Mechatron. 24 (5), 2215–2226. https://doi.org/10.1109/TMECH.2019.2932312.

Zihajehzadeh, S., Park, E.J., Song, H., 2016. Regression model-based walking speed estimation using wrist-worn inertial sensor. PLoS ONE 11 (10), e0165211. https://doi.org/10.1371/journal.pone.0165211.